Hindawi
Geofluids
Volume 2022, Article ID 9420835, 10 pages
https://doi.org/10.1155/2022/9420835

Research Article

Characterization Method of Tight Sandstone Reservoir Heterogeneity and Tight Gas Accumulation Mechanism, Jurassic Formation, Sichuan Basin, China

Lin Jiang,[1] **Wen Zhao**,[1] **Benjian Zhang**,[2] **Chao Zheng**,[2] **Feng Hong**,[1] **and Jiaqing Hao**[1]

[1]*Research Institute of Petroleum Exploration and Development, PetroChina, Beijing 100083, China*
[2]*Research Institute of Petroleum Exploration and Development, Southwest Oilfield, PetroChina, Chengdu 610000, China*

Correspondence should be addressed to Wen Zhao; zhaow625@126.com and Benjian Zhang; zbjian@petrochina.com.cn

Received 6 April 2022; Revised 11 May 2022; Accepted 27 June 2022; Published 20 July 2022

Academic Editor: Chao-Zhong Qin

Although significant progress has been made in tight gas exploration and development, there is still a limited understanding of the gas accumulation mechanism in tight formation. The description of heterogeneity in the tight reservoir is still an obstacle during tight gas exploration. In this work, we will develop a 3D gas accumulation facility that can reflect the high temperature and pressure under the geological condition to simulate the gas accumulation process in the tight formation of the Jurassic Formation, Sichuan Basin. Both the physical experiment simulation and numerical simulation methods will be combined to reveal the mechanism of gas accumulation. The results show that (1) the permeability ratio can characterize the heterogeneity of tight reservoirs. Based on this parameter, petroleum geologists can understand the interlayer heterogeneity during fluvial deposition and predict the sweet spots of tight gas; (2) the permeability ratio relationship between hydrocarbon accumulation of the tight sandstone reservoir mainly manifests as long as there is the existence of the differential permeability and there will be differences in natural gas migration dynamics, so that the natural gas accumulates in pores and depends on the extent of source rock; and (3) although the difference between capillary force curves is at the core of the influence of the permeability ratio on the gas-bearing capacity of the "sweet spot" sand body, the permeability ratio is a parameter of practical engineering significance. This work adds new methods to tight gas formation heterogeneity characterization and sheds light on the mechanisms of hydrocarbon accumulation in tight formation.

1. Introduction

Heterogeneity is an important property of tight reservoirs; however, how to describe the reservoir heterogeneity has always puzzled petroleum geologists [1, 2]. Different from the tight gas deposited in North America, tight continental gas is widely distributed in China. Compared with marine sedimentary strata, continental sedimentary strata are more heterogeneous. As a Chinese petroleum geologist, Qiu [3] proposed a classification criterion for reservoir heterogeneity which gained him an excellent reputation. In this classification frame, reservoir heterogeneity is divided into three categories: (1) plane heterogeneity, which refers to the heterogeneity caused by the geometry, size, and continuity of a reservoir sand body, as well as the spatial variation of porosity and permeability within the sand body [4]; (2) intralayer heterogeneity, which is mainly used to characterize the changes of vertical reservoir properties in a single sand body and is a crucial geological factor controlling and affecting the sweep thickness of the vertical injection agent in a single sand body [5]; and (3) interlayer heterogeneity, which refers to the overall study of the vertical lithology and physical property differences among sand layers in a unit, belonging to the reservoir description of the scale of strata [6]. These three types of heterogeneity are widely used to describe reservoir heterogeneity. However, there are huge differences between tight sandstone reservoirs and conventional reservoirs. The heterogeneous description methods for conventional reservoirs have apparent limitations in the description process for tight sandstone gas reservoirs [7].

Especially for the fluvial tight sandstone gas in Sichuan Basin, people need a novel method that focuses on describing the heterogeneity of the tight sandstone reservoir in the study of the natural gas accumulation process.

Hydrocarbon accumulation simulation is an essential means of petroleum geology theory research. Since the 20th century, with the skyrocketing development of the hydrocarbon exploration theory, hydrocarbon accumulation simulation technology has also gained continuous success, from one-dimensional simulation to three-dimensional simulation [8, 9], from macroscopic basin simulation to microscopic molecular simulation [10], and from normal temperature and pressure simulation to high-temperature and pressure geological simulation [11]. The progress of hydrocarbon accumulation simulation technology also promotes the development and innovation of hydrocarbon migration and accumulation theory. The hydrocarbon accumulation simulation technology development can be divided into three stages: (1) the practical exploration stage from the early 20th century to the middle of the 20th century. In this stage, people mainly used simple physical simulation experiments to verify their theoretical hypotheses [12]. Petroleum geologists propose theoretical hypotheses, then design and build their experimental equipment to carry out experiments according to the mechanism of hydrocarbon migration and accumulation, and rely on the results to support their theoretical hypotheses [13, 14]; (2) from the middle of the 20th century to the end of the 20th century, people began to pay attention to the controlling effects of microscopic parameters such as interfacial tension and pore wettability [15, 16] and throat radius on hydrocarbon migration [17]. With the development of science and technology and petroleum and natural gas geological theory, people began to pay attention to microparameters such as wettability [18], interfacial tension, and pore-throat structure on oil and gas migration in the late 20th century. During this time, hydrocarbon accumulation simulation technology developed from macroscale to micro-scale [19, 20]. (3) The development and innovation stage from the 21st century to the present is also accompanied by the boom of unconventional resources and the birth of many new technologies and methods [21]. In the 21st century, more and more testing equipment and analytical instruments have been applied to petroleum geology. In this stage, people's simulation of the hydrocarbon accumulation process has changed from a normal temperature and pressure environment to a high-temperature and pressure environment closer to geological conditions [22]. With the rapid development of unconventional resources, the mechanism of oil and gas charging and hydrocarbon migration and accumulation at the micro- and nanoscale has become a core scientific issue in the theoretical study of tight oil and gas accumulation. At the same time, reservoir formation simulation technology has also been developed and many new technologies and methods have been applied in this field, such as online nuclear magnetic technology [23] and 3D CT imaging technology [24]. Similarly, with the rapid development of computer technology and algorithms and the digitization process of geological data, it is possible to simulate the process of hydrocarbon accumulation with multiscale, multidimensional, multifactor, large-scale, and whole-process dynamics. More and more numerical simulation methods have been applied to hydrocarbon accumulation simulation [25]. Oil and gas accumulation simulation technology promotes the study of oil and gas accumulation mechanisms and makes up for the lack of theoretical research. Especially in recent years, further breakthroughs have been made in the exploration and development of unconventional global resources.

However, there exist huge differences between conventional resources and unconventional resources; how to establish a set of physical and numerical tight sandstone gas accumulation simulation technology and method that can meet the conditions of underground temperature and pressure according to the characteristics of tight sandstone gas reservoir development becomes a critical technical problem to be solved. In this work, based on the geological background of the Jurassic Formation, Sichuan Basin, we will discuss the cause of the heterogeneity of tight reservoirs and study how to characterize the heterogeneity of tight reservoirs. The physical experiment simulation and numerical simulation will be combined to reveal the mechanism of tight gas accumulation.

The rest of this paper is organized as follows. In Section 2, the geological background of the Jurassic Formation, Sichuan Basin, will be introduced. The cause of heterogeneity of a tight reservoir and the study on how to characterize the heterogeneity of tight reservoirs will be discussed in Section 3. In Sections 4 and 5, the physical experiment simulation and numerical simulation will be combined to reveal the mechanism of tight gas accumulation. A case of field application will be presented in Section 7.

2. Geological Backgrounds

As a significant petroliferous basin, the Sichuan Basin is located at southwest China (Figure 1). The tectonic pattern of the Sichuan Basin is controlled by the alternating thrust and nappe activities of the Longmen Mountain, Micang Mountain-Daba Mountain, and Xuefeng Mountain orogenic belts, and the basin-mountain coupling processes of each depression belt in the basin are strongly staged and transferable.

The mid-late Triassic was the critical period for the tectonic system transformation of the middle and upper Yangtze block. The surrounding ocean basins were subducted and subducted until finally closed. With the closing of the Paleotethys ocean, the vast area of south China underwent large-scale marine backsliding and turned into continental deposition. During the Jurassic sedimentary period, the lacustrine delta and fluvial sedimentary system were mainly developed. The thrust-nappe activity in the Longmen Shan area began to weaken. In contrast, the Micang Mountain-Daba Mountain tectonic activity became intense, making the basin subsidence and sedimentary filling center gradually migrate from the front of Longmen Mountain in western Sichuan to the front of Micang Mountain-Daba Mountain in northern Sichuan.

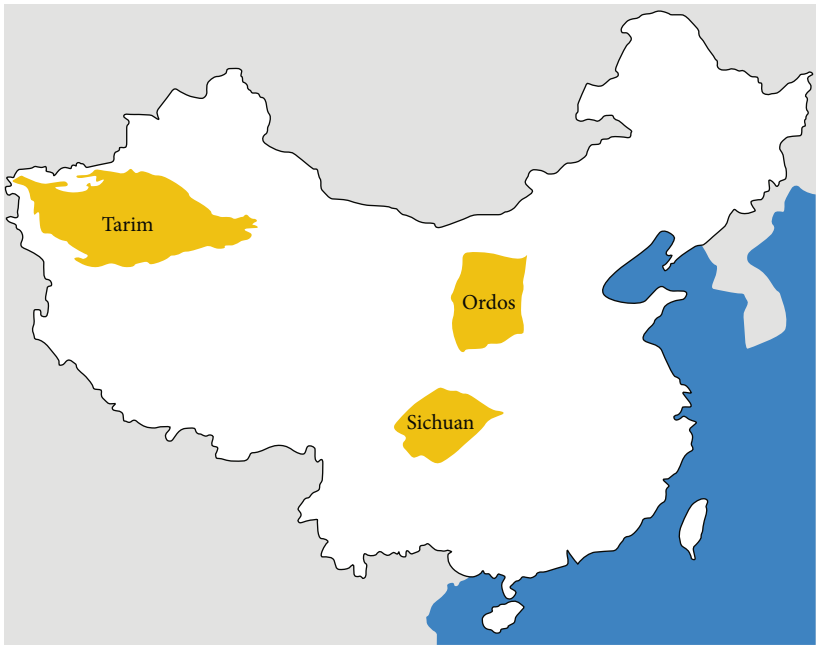

Figure 1: Map of the main sedimentary basins of China.

3. Characterization Method of Tight Sandstone Reservoir Heterogeneity

3.1. Heterogeneity Characteristics. Shaximiao Formation is a set of substantial thick purplish-red mudstone intercalated with the massive sand bodies, which is widely distributed in the basin. During the sedimentary period of the Shaximiao Formation, the detrital supply of Micang Mountain and Daba Mountain was strong, which controlled the provenance system of central Sichuan, and the piedmont provenance system of western Sichuan originated from Longmen Mountain. The channel sand reservoirs of Shaximiao Formation in the basin are well developed and affected by provenance, sedimentary microfacies, and diagenesis; the reservoirs have pronounced zoning and stratification.

The physical properties of different sand groups in different areas are characterized by low porosity-extremely low porosity and extremely low permeability-low permeability. The porosity ranges from 4% to 16%, with an average of 10.07%. Permeability ranges from 0.0018 to 191.338 mD, with an average of 3.45 mD. The fluvial sand group has firm heterogeneity and significant physical property difference between layers. The porosity of each sand group varies significantly from 7.11% to 14.58%. The permeability of each sand group varies greatly from 0.06 to 13.06 mD. Sedimentary microfacies mainly control the intralayer heterogeneity, and the interlayer heterogeneity is mainly controlled by diagenesis. Characterizing the heterogeneity of tight reservoirs and the predicting gas-bearing capacity have become a problem that people must face. This work will use the permeability ratio as a parameter to characterize the heterogeneity of tight reservoirs and discuss its relationship with gas saturation.

3.2. The Concept of the Permeability Ratio. Permeability ratio refers to the ratio of the maximum permeability to the minimum permeability of the rock, indicating the distribution range and difference in permeability [26]. The larger the permeability ratio is, the more substantial the heterogeneity of the reservoir pore space is. The closer to 1, the better the homogeneity of reservoirs.

The permeability ratio reflects the heterogeneity of the reservoir. Its geological meaning includes the following characteristics: (1) due to the influence of various geological processes of sandstone reservoir sedimentation, diagenesis, and later transformation, the permeability ratio varies; (2) the permeability ratio exists all the time; as long as there is heterogeneity in sandstone, the permeability ratio should be a relative concept; and (3) the permeability of sandstone reservoirs generally varies greatly, and there may be significant differences in different measurements of the same lithology. Therefore, the permeability ratio refers to the heterogeneity of rock, which is the characteristic of rock permeability caused by sedimentation, diagenesis, and later transformation. It is a relative concept and can be quantitatively characterized by the ratio of maximum permeability (K_{max}) and minimum permeability (K_{min}).

3.3. Formation of the Permeability Ratio. The permeability ratio essentially reflects the heterogeneity of rock. Primary and later reformations cause the differences in petrophysical properties. The main factors causing the heterogeneity of petrophysical properties are sedimentary environment and diagenesis.

3.3.1. Depositional Environment Difference. The sedimentary environment plays a vital role in the formation of permeability variety, which is mainly manifested in the variability of continental sedimentary facies. Mesozoic and Cenozoic continental

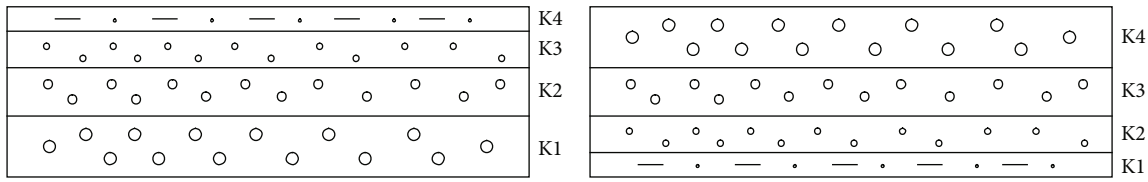

(a) Positive rhythm deposit (b) Negative rhythm deposit

Figure 2: A pattern of permeability differentials formed by sedimentation. (a) The positive rhythm deposit; (b) the negative rhythm deposit. In the positive rhythm deposit model, K1 > K2 > K3 > K4, and in the negative rhythm deposit model, K1 < K2 < K3 < K4.

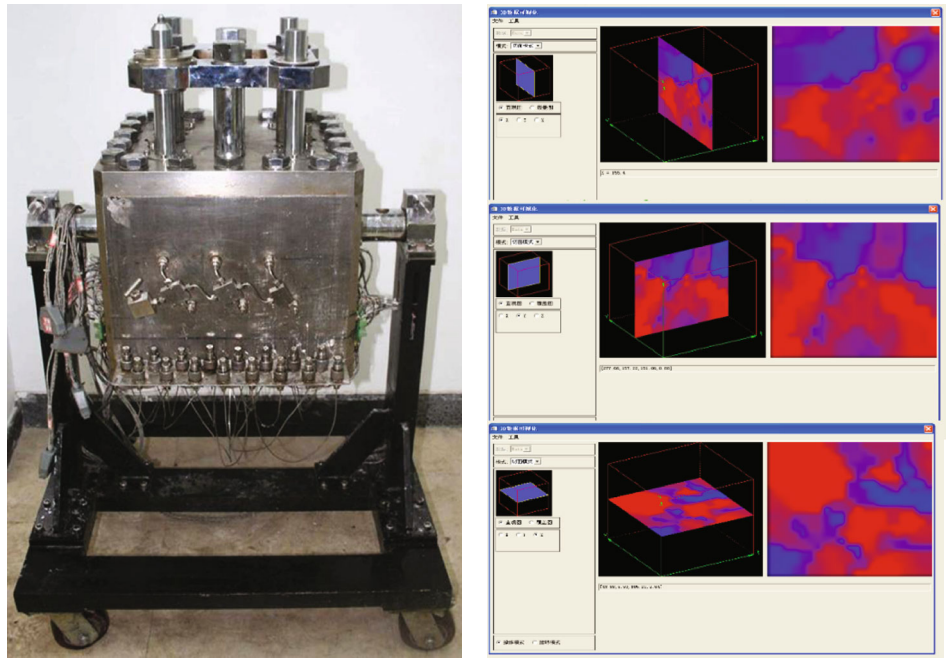

(a) 3D sandbox (b) Data acquisition software

Figure 3: 3D physical simulation facility and data acquisition software. (a) The main body of the 3D sandbox. (b) The distribution of fluids in the sandbox during the experiment process; the red represents the gas phase, and the blue represent the water phase.

sedimentary basins are mainly developed in tight sandstone gas reservoirs in China. Continental sedimentary systems include the alluvial fan system, river system, delta system, lake system, and swamp system, and each system has different sedimentary facies. Therefore, continental sedimentary patterns are variable both vertically and horizontally.

The permeability ratio caused by sedimentary facies can be different sedimentary systems or different sedimentary microfacies. In the longitudinal direction, the sedimentary phase transformation forms are positive rhythm deposition and antirhythm deposition. In the lateral direction, mainly sedimentary facies change, both of which can cause the heterogeneity of sandstone reservoirs in the longitudinal or transverse directions (Figure 2). Positive rhythmic sand is the common feature of various fluvial sedimentary sand bodies for rhythmic deposition. From the bottom to the top of the sandstone, the grain size changes from coarse to fine and the permeability changes from high to low. The permeability ratio in positive rhythm sand varies significantly due to different sedimentation.

3.3.2. Diagenetic Difference. Diagenesis controls the distribution of relatively high permeability zones. The formation has experimence a long period of sedimentation.

Compaction includes mechanicam compaction and pressolution. On the one hand, the pressure solution makes the particles contact more closely. On the other hand, the dissolved material precipitates to fill the intergranular pores or provides much silica for quartz enlargement and silica cementation, so the development of porosity and permeability of the clastic reservoir is more unfavorable. According to the experiment, the porosity loss of clastic rock can be divided into three levels. Class I is weak compaction, the clastic particles are point contact, and the porosity loss of clastic rock is 5%~10%. In class II, the clastic particle contact is linear contact or concave-convex contact and the porosity loss of clastic rock is 10%~15%. In class III, there is strong compaction, the clastic particles disappear obviously, and the porosity loss of clastic rock is 15%~30%. Diagenetic compaction and cementation also control the permeability ratio of clastic reservoirs. Without considering the later reservoir reconstruction, the compaction

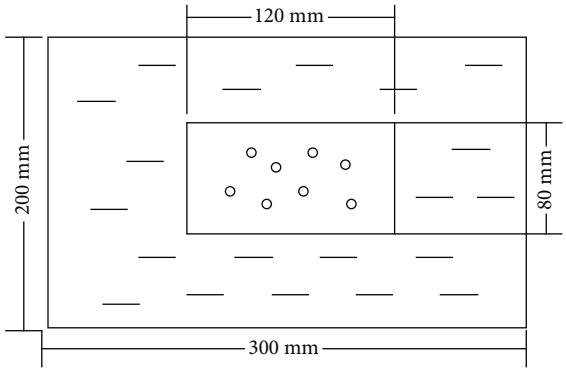

Figure 4: Sand filling model. The middle is a high-permeability sand body, surrounded by a low-permeability sand body.

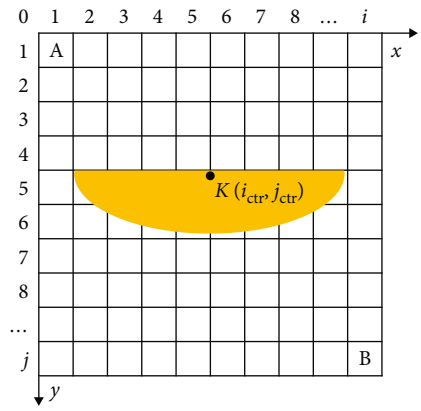

Figure 5: Schematic diagram of the simulation unit. The yellow means the sandstone with better porosity and permeability. The other white area near the yellow area means the sand with lower porosity and permeability [7].

and cementation increase with the increase of burial depth and the porosity and permeability of reservoirs tend to worsen. From the perspective of permeability difference, permeability becomes worse from shallow to deep and reservoirs in the same sedimentary environment also show heterogeneity in the longitudinal direction and there is permeability difference.

3.3.3. Late Reformation Origin. The formation of permeability difference is also caused by late reservoir transformation, leading to the existence of the same reservoir permeability difference. The later reformations are mainly dissolution and tectonism. Dissolution can increase the porosity and permeability of reservoirs. The favorable conditions are as follows: the depositional clastic rocks with coarser grain size and better porosity and permeability. There are many soluble substances in sandstone. Groundwater is acidic and has a specific flow rate. For example, clastic rock reservoirs in coal measures in China generally produce large numbers of organic acids and form an acidic formation water environment, which makes it challenging to form carbonate cementation in the early stage and is conducive to the development of intergranular micropores, thus contributing to porosity. Many tight sandstone gas reservoirs in China belong to coal measures.

The tectonic movement controls the sequence-sedimentary types and some diagenetic conditions and plays an indirect role in controlling the reservoir's physical properties; especially for fractured reservoirs, the structure is a direct control factor. Fractures and microfractures generated by structures can increase reservoir space and greatly improve permeability and serve as a significant channel for pore water transport. Fracture development can accelerate dissolution. Fractures have a great impact on reservoir and productivity in tight reservoirs, thus directly determining reservoir productivity.

The late structural transformation is mainly due to the extrusion of tectonic stress, the axial part of an anticline or the core of paleo-uplift is formed because of the fracture, and the permeability becomes better, often showing the characteristics of the axial wing permeability decreases, resulting in the existence of permeability level difference.

4. Physical Experiment Simulation of Tight Gas Accumulation

The experiment simulations of hydrocarbon migration and accumulation are mainly based on sandbox facilities. However, the typical sandbox experiment cannot restore the temperature and pressure conditions of the formation. In this section, we will develop a novel 3D sandbox facility that can restore the real reservoir's temperature and pressure condition.

4.1. Experimental Facility. The 3D sandbox experimental facility can be divided into two parts: the hardware part and the software part. Figure 3 shows both parts of the 3D physical sandbox simulation facility and date acquisition software.

Figure 3(a) shows the hardware part. The internal scale of the sandbox is $300 \times 300 \times 200$ mm; 128 electrodes and 12 temperature and pressure sensors are placed inside the sandbox. The sensors are uniformly distributed in the model in three dimensions to monitor the fluid migration and accumulation process. The electrode is in direct contact with the fluids in the sandbox, and the resistivity is used to determine whether the fluid at the vicinity of the measurement point is gas or water. The distribution characteristics of the fluid in the sandbox are obtained from the measurement point data of 128 electrodes.

There are significant differences in resistivity between the water and gas phases. Differences in resistivity will result in differences in the measured current value during the experiment. When the fluid near the measuring electrode is gas, the resistance measured is higher and the current measured is lower. When the fluid near the measuring electrode is water, the resistance measured is lower and the current measured is higher. Based on 128 measuring points we can obtain the fluid distribution characteristics of sandbox under high temperature and high pressure (Figure 3(b)).

4.2. Process of the Experiment. The primary process of the experiment is as follows.

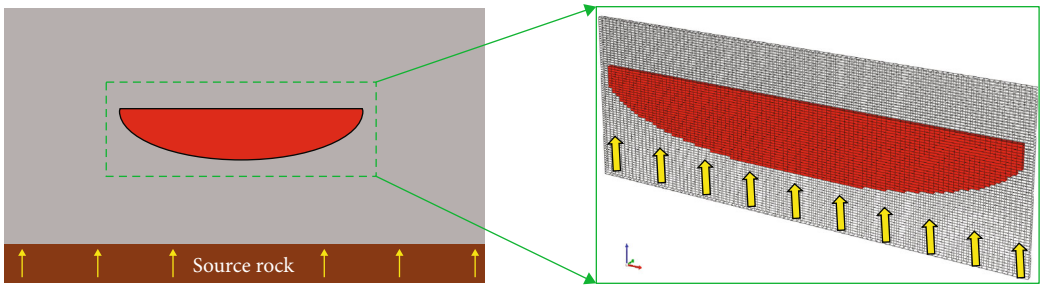

Figure 6: The numerical simulation process. The red means the center sand which has better porosity and permeability, the yellow means the gas, which migrate into the sand, and the size of cell is 0.5 m × 0.5 m [7].

Table 1: The properties of samples used in the capillary curve tests.

Sample	Porosity (%)	Permeability (mD)	Mercury injection curve (MIC)
No. 1	1.11	0.015	MIC-1
No. 2	3.69	0.028	MIC-2
No. 3	7.59	0.26	MIC-3
No. 4	10.31	2.62	MIC-4

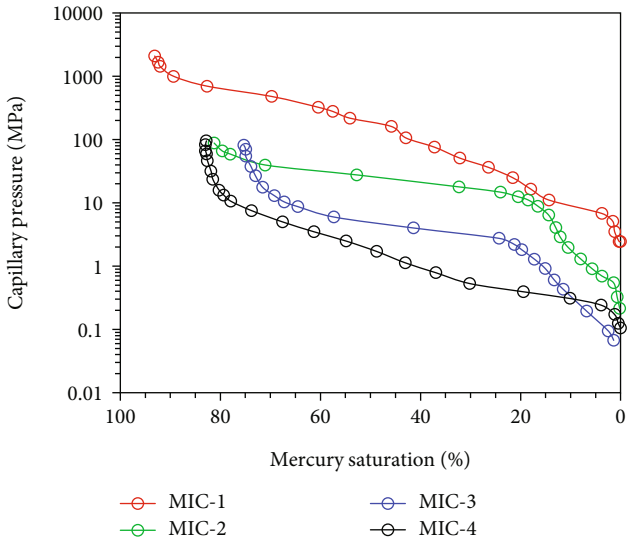

Figure 7: The capillary curves of four samples used in the numerical simulation process. The x-axis shows the injected mercury saturation, and the y-axis shows the capillary pressure. Through simple conversion, the pressure can be converted to capillary pressure in the presence of gas-water two-phase fluid.

Assemble equipment and install electrodes. Glass beads with different particle sizes were selected for experimental model filling. The electrodes of glass beads with different permeability were calibrated. Figure 4 shows the sand filling mode; the middle is a high-permeability sand body, surrounded by a low-permeability sand body.

The formation water is injected from the top cover of the mold by a dynamic injection system, and the sandstone body is compacted at the pressure of 9 MPa.

When the model is compacted, connect the electrode and pressure sensor circuit, move the whole model to the thermostat, and set the temperature of the thermostat at 90°C.

Run monitoring software, input physical experiment parameters, and start real-time data collection software.

The model was first saturated with water, and gas was injected from the bottom of the model at a stable pressure of 4.5 MPa for 13 days, and the experiment ended. The gas charging process is monitored in real time using the saturation measuring electrode. The phase distributions are given in Section 6.

As shown in Figure 4, in order to simulate the permeability heterogeneity of formation, the permeability of the middle permeability sand body is 300 mD and the permeability of the surrounded sand body is 100 mD, although the permeability of the physical model is higher than the actual tight formation. We want to use this model to simulate the permeability heterogeneity of formation, and this model can meet our requirements.

5. Numerical Simulation of Tight Gas Accumulation

In our previous work, we established a numerical simulation method for the tight gas reservoir; in this work, we will extend our previous work [7] and combine our numerical method with the physical experiment method in Section 4. Specific geological modeling methods and numerical simulation methods can be referred to our previously published literature. We only introduced the main methods and process of numerical simulation in this work. Figure 5 shows the schematic diagram of the numerical simulation unit, and the geological model is established as follows:

Assign coordinates to each grid in sequence (i, j).

Different sand bodies are numbered by the K value, and the top center of the central sand body is (i_{ctr}, j_{ctr}).

The control function formula (x, y, i_{ctr}, j_{ctr}) is used to describe the sand body morphology.

Judge whether the coordinate of any cell falls in the control formula. If it falls within the range of the sand body control formula, assign the value of the sand body to the cell. If the unit is not within the range of the control formula, the outer tight sandstone is assigned to the unit.

Table 2: Parameters for simulations.

	Parameters for center body			Parameters for surrounding sandstones		
	Porosity (%)	Permeability (mD)	MIC	Porosity (%)	Permeability (mD)	MIC
Simulation 1	3.69	0.028	MIC-2	1.11	0.015	MIC-1
Simulation 2	7.59	0.26	MIC-3	1.11	0.015	MIC-1
Simulation 3	10.31	2.62	MIC-4	1.11	0.015	MIC-1

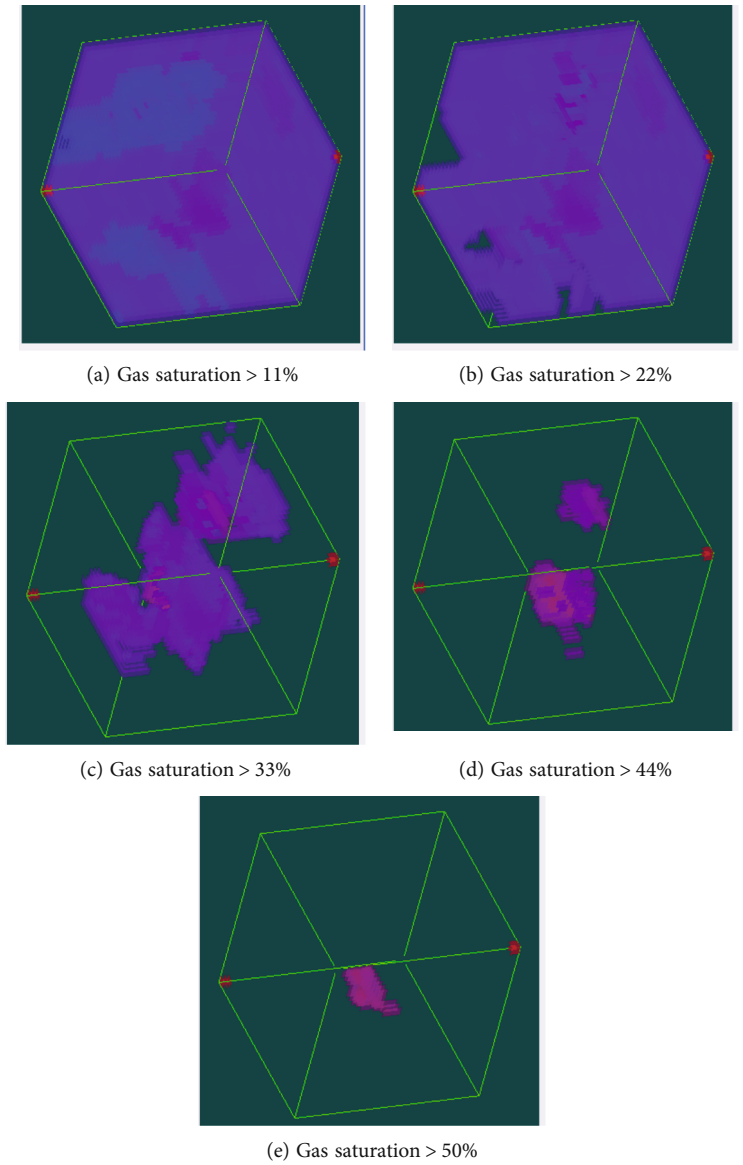

(a) Gas saturation > 11%

(b) Gas saturation > 22%

(c) Gas saturation > 33%

(d) Gas saturation > 44%

(e) Gas saturation > 50%

Figure 8: The gas saturation distribution of physical experiment simulation. From blue to red indicates a gradual increase in gas saturation. (a) Shows the gas saturation distribution, which is greater than 11%, and (e) omits the area with gas saturation of less than 55%.

After several cycles, each grid is assigned corresponding values to complete the resume of the geological model.

Figure 6 shows the numerical model used in this work which is similarly to the physical experiment model used in Section 4. This geological model is imported to the simulator CMG platform. Natural gas is charged from bottom to top. The red is the high-porosity and high-permeability sand body, and the gray part is the tight sandstone around the sand body. During the charging process, the natural gas from the source rock migrates to the sand body and accumulates in the sand body in the center.

During the numerical simulation process, the rock properties of the different sand bodies, such as porosity, permeability, and capillary curve, are from the natural rock sample of the

Table 3: Numerical simulation results.

	Pore volume of center sand body (m^3)	Gas saturation (%)	Reserve ($\times 10^4\ m^3$)
Simulation 1	3192.9	0.46	71
Simulation 2	5565.1	0.53	164
Simulation 3	8656.4	0.67	211

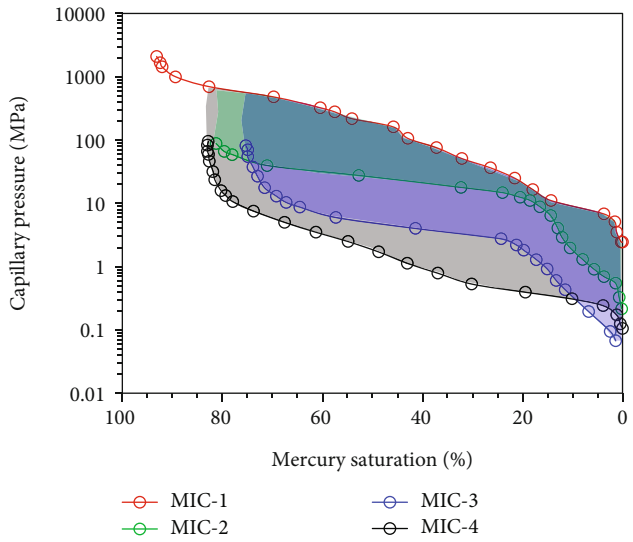

Figure 9: Capillary force curves for the four samples used in the simulations. As the surrounding rock, sample 1 has the highest capillary pressure of four samples and the other three capillary curves can enclose areas with the capillary curve of the surrounding rock. Three areas can be observed in this figure. Different colors distinguish them; the green area represents the capillary pressure difference between sample 1 and sample 2, which is used as the surrounding rock and center sandy body of simulation 1. The blue and the black areas represent simulation 2 and simulation 3.

tight formation. Table 1 shows the properties of four samples used in the numerical simulation process. The most crucial property of capillary curves is tested by the mercury injection method. Figure 7 shows the capillary curves of four samples used in the numerical simulation process. Through simple conversion, the pressure can be converted to capillary pressure in the presence of gas-water two-phase fluid.

Table 2 shows the used parameters for simulations in this work. During the numerical simulation process, sample 4 represents the surrounding rocks around the center sand body.

6. Results and Discussion

Figure 8 shows the results of the physical experiment simulation of Section 4. From blue to red indicates a gradual increase in gas saturation. The permeability difference of sandstone directly affects the gas-bearing property of tight sandstone reservoirs; the central sand body has the highest gas saturation. Heterogeneity is an essential feature of tight sandstone reservoirs. According to the understanding of the origin of permeability difference, the factors causing heterogeneity of tight sandstone reservoirs are original, mainly referring to the difference in permeability caused by the difference of sedimentary diagenesis, which is mainly reflected in the heterogeneity between layers. The other is the late transformation factor, which is the same sandstone reservoir, due to the late uneven dissolution, and structural fractures caused by the emergence of local high-permeability reservoirs, mainly manifested in the layer heterogeneity.

Due to the heterogeneity of tight sandstone, oil and gas migration and accumulation in sand bodies are different. During the migration of oil and gas in clastic reservoirs, the main driving forces are pressure and buoyancy. According to some scholars' research, the migration of natural gas in sandstone is mainly the function of buoyancy and capillary force.

Gas from the source rocks migrates into the capillary pore structure of the sandstone reservoir. Natural gas will accumulate under the barrier layer and accumulate into reservoirs if there is a barrier layer. In this process, the migration trend of natural gas is from the capillary pore structure to the conventional pore structure. The natural gas migration always migrates and accumulates along the reservoir with good porosity and permeability. For the heterogeneous sandstone with permeability difference, the oil and gas migration first points to the reservoir with good permeability.

Table 3 shows the results of the numerical simulation in Section 5. Compared to the physical simulation, the numerical simulation can simulate the high-temperature and pressure condition of actual formation and the reserve can be estimated in quantity. From simulation 1 to simulation 3, the permeability ratio becomes more extensive, which means that the heterogeneity of formation becomes stronger.

Figure 9 shows the capillary pressure difference between the center sand body and surrounding rock. The area enclosed by the capillary curves of the center sand body and surrounding rock shows the capillary pressure difference between the center sand body and surrounding rock. The larger the area is, the more significant the capillary pressure difference between the center sand body and surrounding rock, which represents that the more heterogeneous the formation is. As shown in Figure 9, the black area represents the capillary difference between sample 1 and sample 4; the green area represents the capillary difference between sample 1 and sample 2, and the black area is more extensive.

Through the abovementioned simulation and discussion, it can be observed that the difference in gas content caused by permeability level difference in simulations 1, 2, and 3 is, in essence, caused by the difference in capillary force between the center sand body and tight surrounding rock. In the charging process, when the natural gas enters the center sand body, the more significant the difference of capillary force between the center sand body and the tight

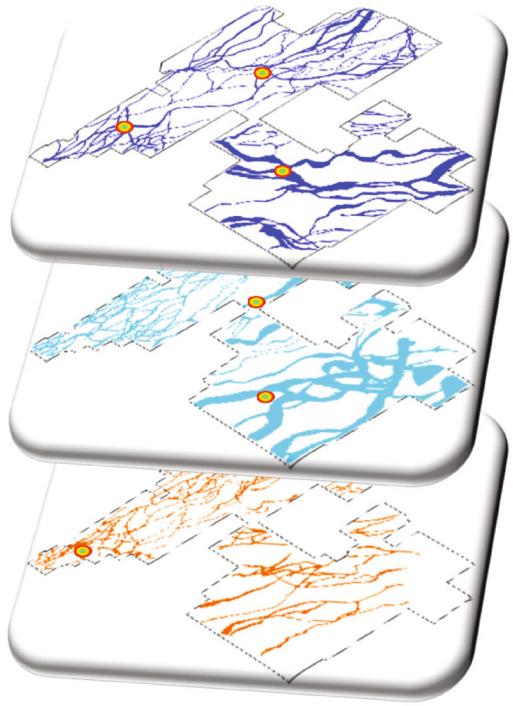

Figure 10: Multistage channel distribution model of Shaximiao Formation, Jurassic in the Sichuan Basin. Different colors indicate different periods.

surrounding rock, the easier the natural gas will accumulate in the "sweet spot" sand body. However, although the difference between capillary force curves is at the heart of the influence of permeability difference on the gas-bearing capacity of center sand, the parameter permeability difference is still of practical significance.

Generally, the lower the permeability, the greater the capillary force of the reservoir and the greater the permeability level difference can also reflect the more extraordinary capillary force difference between the center sand body and the tight surrounding rock. The permeability differential is much easier to obtain than the differential characterization of capillary forces. Some researchers used the permeability difference between the sweet spot and surrounding rock to judge the critical condition of gas accumulation. When the permeability difference is higher than the critical ratio, the gas is favorable to accumulate in the center sand body. If the ratio is less than the critical ratio, it becomes difficult for the gas to accumulate in the center sand body. The pore structure is complicated in the underground reservoir, so more attention should be paid to the capillary pressure difference between the sweet spot and surrounding rock to judge whether the gas can accumulate in the sweet spot.

The charging process of natural gas in sand bodies under different pore and permeability conditions. (1) When the natural gas generated from source rock enters tight sandstone, it must overcome the capillary force in the capillary pore structure to enter the reservoir; (2) the relatively high permeability of tight sandstone reservoir sand body (lens) capillary force primary does not exist; natrual gas migrates from sand body with low permeability to sand body with high permeability; natural gas accumulates in the upper area of sand body; (3) with the continuous charging of natural gas, the high-porosity and permeability sand body is filled with natural gas, forming a local gas-rich collective.

7. Field Application

The exploration of Jurassic tight gas in Sichuan Basin began in 1977 and went through three stages: gas generation exploration, lithologic gas exploration, and tight gas exploration and development stage.

(1) Early structural trap exploration stage (1977–1996). In this stage, petroleum geologists discovered the Daxingchang gas reservoir in southwest Sichuan

(2) Lithologic gas reservoirs in structural area stage (1997–2017). In this stage, Pingluoba, Yanjinggou, and Baima Temple gas reservoirs were found in southwest Sichuan, the Wubaochang gas reservoir was found in northeast Sichuan, and the Datachang gas reservoir in south Sichuan was discovered

(3) Tight gas exploration stage (2018–present). According to the abovementioned analysis, the essence of the gas accumulation in the tight formation is the heterogeneity of the reservoir. The permeability ratio can well describe the heterogeneity of the formation. Under the guidance of this geological theory, during the tight gas exploration stage, petroleum geologists discovered Qiulin and Bajiaochang multistage gas-bearing sand groups in central Sichuan; the PetroChina Company proved reserves of 9.462 billion cubic meters, and 17.686 billion cubic meters was submitted. The middle Sichuan Basin can be divided into 23 periods of channel sand groups from bottom to top longitudinally, and 13 periods are found to contain gas. Figure 10 shows the multistage channel distribution model of Jurassic in the Sichuan Basin. Different colors indicate different periods. The colorful points show the exploration wells with high production; they are located in the sand bodies, which have high permeability which has a higher permeability ratio

8. Conclusions

The permeability ratio can well characterize the heterogeneity of tight reservoirs. Based on this parameter, petroleum geologists can understand the interlayer heterogeneity during fluvial deposition and predict the sweet spots of tight gas.

The permeability ratio relationship between hydrocarbon accumulation of the tight sandstone reservoir mainly manifests as long as there is the existence of the differential permeability and there will be differences in natural gas migration dynamics, so that the natural gas accumulates in pores and depends on the extent of source rock.

The difference in gas saturation caused by the permeability ratio is caused by the difference in capillary force between the center sand body and the tight surrounding rock. The

permeability ratio is a parameter of practical engineering significance.

Data Availability

All supporting data can be found in the manuscript.

Conflicts of Interest

The authors declare that they have no conflicts of interests.

Acknowledgments

This work was supported by the CNPC Scientific Research and Technology Development Project "whole petroleum system theory and unconventional hydrocarbon accumulation mechanism" (2021DJ0101).

References

[1] R. Kadkhodaie-Ilkhchi, A. Kadkhodaie, R. Rezaee, and V. Mehdipour, "Unraveling the reservoir heterogeneity of the tight gas sandstones using the porosity conditioned facies modeling in the Whicher Range field, Perth Basin, Western Australia," *Journal of Petroleum Science and Engineering*, vol. 176, pp. 97–115, 2019.

[2] L. Huang, W. Zhou, H. Xu, L. Wang, J. Zou, and Q. Zhou, "Dynamic fluid states in organic-inorganic nanocomposite: implications for shale gas recovery and CO_2 sequestration," *Chemical Engineering Journal*, vol. 411, p. 128423, 2021.

[3] Y. Qiu, "Geological methodology of petroleum development (I)," *Petroleum Exploration and Development*, vol. 23, no. 2, pp. 43–47, 1996.

[4] P. Avseth, T. Mukerji, G. Mavko, and J. Dvorkin, "Rock-physics diagnostics of depositional texture, diagenetic alterations, and reservoir heterogeneity in high-porosity siliciclastic sediments and rocks—a review of selected models and suggested work flows," *Geophysics*, vol. 75, no. 5, p. 75A31-75A47, 2010.

[5] M. Venieri, S. J. Mackie, S. H. McKean et al., "The interplay between cm- and m-scale geological and geomechanical heterogeneity in organic-rich mudstones: implications for reservoir characterization of unconventional shale plays," *Journal of Natural Gas Science and Engineering*, vol. 97, article 104363, 2022.

[6] K. Alam, O. Abdullatif, A. El-Husseiny, and L. Babalola, "Depositional and diagenetic controls on reservoir heterogeneity and quality of the Bhuban Formation, Neogene Surma Group, Srikail Gas Field, Bengal Basin, Bangladesh," *Journal of Asian Earth Sciences*, vol. 223, p. 104985, 2022.

[7] W. Zhao, T. Zhang, C. Jia, X. Li, K. Wu, and M. He, "Numerical simulation on natural gas migration and accumulation in sweet spots of tight reservoir," *Journal of Natural Gas Science and Engineering*, vol. 81, p. 103454, 2020.

[8] W. Zhao, C. Jia, L. Jiang et al., "Fluid charging and hydrocarbon accumulation in the sweet spot, Ordos Basin, China," *Journal of Petroleum Science and Engineering*, vol. 200, p. 108391, 2021.

[9] W. Zhu, Y. Liu, Y. Shi, G. Zou, Q. Zhang, and D. Kong, "Effect of dynamic threshold pressure gradient on production performance in water-bearing tight gas reservoir," *Advances in Geo-Energy Research*, vol. 6, no. 4, pp. 286–295, 2022.

[10] W. Zhao, C. Jia, T. Zhang et al., "Effects of nanopore geometry on confined water flow: a view of lattice Boltzmann simulation," *Chemical Engineering Science*, vol. 230, p. 116183, 2021.

[11] L. Jiang, W. Zhao, J. Huang, Y. Fan, and J. Hao, "Effects of interactions in natural gas/water/rock system on hydrocarbon migration and accumulation," *Scientific Reports*, vol. 11, no. 1, pp. 1–13, 2021.

[12] M. J. Munn, "The anticlinal and hydraulic theories of oil and gas accumulation," *Economic Geology*, vol. 4, no. 6, pp. 509–529, 1909.

[13] W. C. Gussow, "Differential entrapment of oil and gas: a fundamental principle," *AAPG Bulletin*, vol. 38, no. 5, pp. 816–853, 1954.

[14] Z. Sun, B. Huang, K. Wu et al., "Nanoconfined methane density over pressure and temperature: wettability effect," *Journal of Natural Gas Science and Engineering*, vol. 99, p. 104426, 2022.

[15] B. Pan, Y. Li, H. Wang, F. Jones, and S. Iglauer, "CO2and CH4wettabilities of organic-rich shale," *Energy & Fuels*, vol. 32, no. 2, pp. 1914–1922, 2018.

[16] B. Pan, F. Jones, Z. Huang et al., "Methane (CH4) wettability of clay-coated quartz at reservoir conditions," *Energy & Fuels*, vol. 33, no. 2, pp. 788–795, 2019.

[17] R. Lenormand, E. Touboul, and C. Zarcone, "Numerical models and experiments on immiscible displacements in porous media," *Journal of Fluid Mechanics*, vol. 189, pp. 165–187, 1988.

[18] B. Pan, X. Yin, Y. Ju, and S. Iglauer, "Underground hydrogen storage: influencing parameters and future outlook," *Advances in Colloid and Interface Science*, vol. 294, p. 102473, 2021.

[19] X. Luo, "Simulation and characterization of pathway heterogeneity of secondary hydrocarbon migration," *AAPG Bulletin*, vol. 95, no. 6, pp. 881–898, 2011.

[20] B. Pan, T. Ni, W. Zhu et al., "Mini review on wettability in the methane–liquid–rock system at reservoir conditions: implications for gas recovery and geo-storage," *Energy & Fuels.*, vol. 36, no. 8, pp. 4268–4275, 2022.

[21] J. R. Boles, P. Eichhubl, G. Garven, and J. Chen, "Evolution of a hydrocarbon migration pathway along basin-bounding faults: evidence from fault cement," *AAPG Bulletin*, vol. 88, no. 7, pp. 947–970, 2004.

[22] D. Connolly, A. Lakhlifi, K. Rimaila et al., "Visualizing hydrocarbon migration pathways associated with the Ringhorne oil field, Norway: an integrated approach," *Interpretation*, vol. 10, no. 1, pp. SB27–SB37, 2022.

[23] T. K. Karamanos and G. M. Clore, "Large chaperone complexes through the lens of nuclear magnetic resonance spectroscopy," *Annual Review of Biophysics*, vol. 51, no. 1, pp. 223–246, 2022.

[24] M. Blunt, L. Kearney, A. Alhosani, Q. Lin, and B. Bijeljic, "Wettability characterization from pore-scale images using topology and energy balance with implications for recovery and storage," in *In SPE Annual Technical Conference and Exhibition*, OnePetro, 2021, September.

[25] Z. Chen, Q. Guo, C. Jiang et al., "Source rock characteristics and rock-eval-based hydrocarbon generation kinetic models of the lacustrine Chang-7 shale of Triassic Yanchang Formation, Ordos Basin, China," *International Journal of Coal Geology*, vol. 182, pp. 52–65, 2017.

[26] E. P. Weeks, "Determining the ratio of horizontal to vertical permeability by aquifer-test analysis," *Water Resources Research*, vol. 5, no. 1, pp. 196–214, 1969.